SCISPACE
formerly Typeset

Open access • Journal Article • DOI:10.1038/NATURE02732

The principle of temperature-dependent gating in cold- and heat-sensitive TRP channels — Source link

Thomas Voets, Guy Droogmans, Ulrich Wissenbach, Annelies Janssens ...+2 more authors

Institutions: Katholieke Universiteit Leuven, Saarland University

Published on: 12 Aug 2004 - Nature (Nature Publishing Group)

Topics: Gating, Transient receptor potential channel, Ion channel, TRPM Cation Channels and Icilin

Related papers:

- The capsaicin receptor: a heat-activated ion channel in the pain pathway
- Identification of a cold receptor reveals a general role for TRP channels in thermosensation
- A TRP Channel that Senses Cold Stimuli and Menthol
- ANKTM1, a TRP-like Channel Expressed in Nociceptive Neurons, Is Activated by Cold Temperatures
- Clues to understanding cold sensation: Thermodynamics and electrophysiological analysis of the cold receptor TRPM8

Share this paper:

View more about this paper here: https://typeset.io/papers/the-principle-of-temperature-dependent-gating-in-cold-and-4e1io5gvuh

The principle of temperature-dependent gating in cold- and heat-sensitive TRP channels

Thomas Voets[1], Guy Droogmans[1], Ulrich Wissenbach[2], Annelies Janssens[1], Veit Flockerzi[2] & Bernd Nilius[1]

[1]*Laboratory of Physiology, Campus Gasthuisberg, KU Leuven, B-3000 Leuven, Belgium*
[2]*Experimentelle und Klinische Pharmakologie und Toxikologie, Medizinische Fakultät, Universität des Saarlandes, D-66421 Homburg, Germany*

The mammalian sensory system is capable of discriminating thermal stimuli ranging from noxious cold to noxious heat. Principal temperature sensors belong to the TRP cation channel family, but the mechanisms underlying the marked temperature sensitivity of opening and closing ('gating') of these channels are unknown. Here we show that temperature sensing is tightly linked to voltage-dependent gating in the cold-sensitive channel TRPM8 and the heat-sensitive channel TRPV1. Both channels are activated upon depolarization, and changes in temperature result in graded shifts of their voltage-dependent activation curves. The chemical agonists menthol (TRPM8) and capsaicin (TRPV1) function as gating modifiers, shifting activation curves towards physiological membrane potentials. Kinetic analysis of gating at different temperatures indicates that temperature sensitivity in TRPM8 and TRPV1 arises from a tenfold difference in the activation energies associated with voltage-dependent opening and closing. Our results suggest a simple unifying principle that explains both cold and heat sensitivity in TRP channels.

Mammals sense ambient temperature through primary afferent sensory neurons of the dorsal root and trigeminal ganglia[1,2]. These cells convey thermal information from peripheral tissues to the spinal cord and brain, where the signals are integrated and interpreted, resulting in appropriate reflexive and cognitive responses. The mammalian sensory system is capable of detecting and discriminating thermal stimuli over a broad temperature spectrum, ranging from noxious cold (<8 °C) to noxious heat (>52 °C), which implies the existence of different types of temperature sensors with distinct thermal sensitivities[2]. Accumulated evidence suggests that the principal temperature sensors in the sensory nerve endings of mammals belong to the transient receptor potential (TRP) superfamily of cation channels[3,4]. At present, six temperature-sensitive TRP channels (or thermoTRPs)[2] have been described, that together cover almost the entire range of temperatures that mammals are able to sense. Four TRP channels belonging to the TRPV subfamily are activated by heating, with characteristic activation temperatures ranging from warm temperatures (>25 °C for TRPV4; >31 °C for TRPV3)[5–9] to heat (>43 °C for TRPV1)[10] and noxious heat (>52 °C for TRPV2)[11]. TRPM8 and TRPA1 (ANKTM1) are activated by cooling, (<28 °C for TRPM8; <18 °C for TRPA1)[12–14]; although the cold-sensitivity of TRPA1 has been disputed[15].

The origin of the remarkably steep temperature sensitivity of the thermoTRPs is still obscure. Until now, three possible mechanisms for temperature-dependent channel gating have been envisaged[3]. Changes in temperature could lead to the production and binding of channel-activating ligands. Alternatively, the channel protein may undergo temperature-dependent structural rearrangements leading to channel opening. Finally, thermoTRPs may be able to sense changes in membrane tension due to temperature-dependent lipid bilayer rearrangements. However, direct experimental evidence supporting any of these mechanisms is currently lacking.

TRP channels were originally considered as cation channels with little or no voltage sensitivity. This view was in line with the paucity of positively charged residues in the fourth transmembrane domain (S4) (ref. 3), which is known to function as (part of) the voltage sensor in classical voltage-gated K^+, Na^+ and Ca^{2+} channels[16]. Nevertheless, recent studies have demonstrated that TRPM4 and TRPM5, two closely homologous monovalent cation channels, are dually gated by intracellular Ca^{2+} and membrane depolarization[17–19]. Given that the cold- and menthol-sensitive TRPM8 is closely related to TRPM4 and TRPM5, with more than 40% similarity at the amino acid level, we investigated whether it displays similar voltage dependence and whether this might be related to its cold sensitivity.

Cold activation of TRPM8

In whole-cell patch-clamp experiments, cooling to 15 °C (Fig. 1a) or application of the cooling agent menthol (Fig. 1b) activated a robust current in human embryonic kidney (HEK) 293 cells transiently transfected with TRPM8, in line with previous reports[12,13]. Non-transfected or vector-transfected cells were unresponsive to either stimulus. Activation of macroscopic TRPM8 currents by cold and menthol also occurred in cell-free inside-out patches (Fig. 1c, d; data not shown), demonstrating that these stimuli function in a membrane-delimited manner. It should be noted that the temperature-sensitivity of TRPM8 in inside-out patches was shifted towards lower temperatures when compared to whole-cell measurements, which could be due to the loss of a regulatory factor.

A typical feature of TRPM8 currents is the pronounced outward rectification (Fig. 1a–d). Rectification could either be an intrinsic property of the pore or alternatively reflect a voltage-dependent mechanism that closes the channel at negative potentials. Evidence for the latter mechanism was obtained using a classical tail current protocol (Fig. 1e): TRPM8 activates upon depolarization to +120 mV and rapidly closes at negative voltages. Notably, the current–voltage relation obtained immediately after the prepulse to +120 mV was linear (Fig. 1f), indicating that open TRPM8 channels display an ohmic current–voltage relation. The time-dependent closure of TRPM8 at negative potentials persisted when Ca^{2+} and Mg^{2+} were omitted from the intra- and extracellular solutions, excluding block by divalent cations as a cause of rectification (data not shown). Taken together, our data demonstrate that TRPM8 is a voltage-dependent channel activated by membrane depolarization. Outward rectification arises from the rapid and voltage-dependent closure of the channel at negative voltages.

Next, we asked how the voltage dependence of TRPM8 relates to its function as a cold receptor[12,13]. To address this, we tested whether

©2004 Nature Publishing Group

membrane voltage influences the cold sensitivity of the channel by measuring current activation at different holding potentials during slow cooling of TRPM8-expressing cells. During such cooling protocols we consistently found that current activation at depolarized potentials precedes that at more negative potentials (Fig. 2a, b). At +100 mV, robust outward currents were already activated at 32 °C (1,080 ± 230 pA ($n = 12$) versus 69 ± 20 pA ($n = 10$) in non-transfected cells; $P < 0.001$), whereas inward currents at −80 mV were only discernible upon cooling below ~25 °C (Fig. 2a, b). Thus, the cold sensitivity of TRPM8 strongly depends on the transmembrane voltage.

Using a voltage step protocol ranging from −120 to +160 mV (and in some cases up to +220 mV), we determined how temperature affects the voltage dependence of TRPM8 (Fig. 2c). At 37 °C, significant outward currents could only be measured at potentials above +100 mV, and the midpoint voltage of activation ($V_{1/2}$) was around +200 mV (Fig. 2c–e). Cooling induced a leftward shift of the activation curve resulting in channel activity at more physiological voltages: $V_{1/2}$ decreased by approximately 150 mV upon cooling from 37 to 15 °C (7.3 mV °C^{-1}), and saturated around +25 mV between 5 and 10 °C (Fig. 2e). From this we conclude that cooling activates TRPM8 by causing a drastic shift of the voltage dependence of activation.

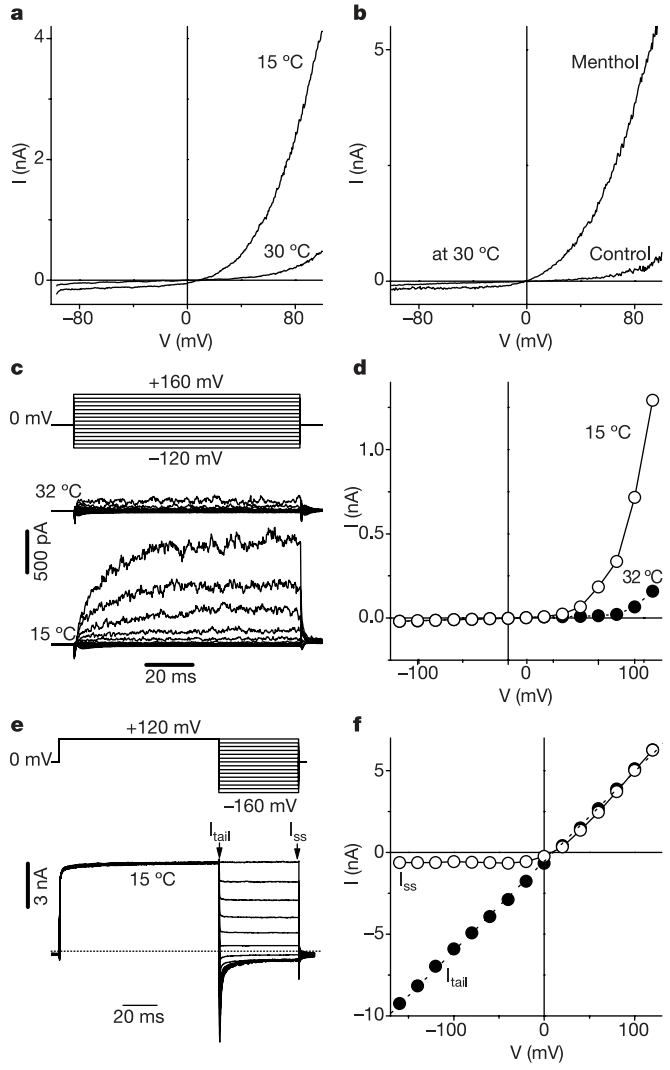

Figure 1 Outward rectification of TRPM8 is due to voltage-dependent gating. **a**, **b**, Current–voltage (I–V) relations of whole-cell TRPM8 currents activated by cooling (**a**) or application of 100 μM menthol (**b**). Currents were measured during 200-ms voltage ramps from −100 to +100 mV. **c**, Effect of cooling on TRPM8-currents measured in inside-out patches. **d**, I–V relations obtained at the end of the voltage-steps shown in **c**. **e**, Whole-cell TRPM8 currents at 15 °C in response to the indicated voltage protocol. **f**, Tail (I_{tail}) and steady-state (I_{ss}) currents obtained from the voltage-steps shown in **e**. The dashed line represents a linear fit.

Heat activation of TRPV1

To test whether a comparable process underlies temperature-dependent gating in a TRP channel with opposite temperature sensitivity, we performed similar experiments in HEK 293 cells expressing TRPV1 (ref. 10). Although TRPV1 was originally described as voltage-independent[10], some voltage-dependent properties of the channel have been recently described[20,21]. During slow heating ramps, we observed that activation of TRPV1 at depolarized voltages occurred at significantly lower temperatures than at hyperpolarized voltages (Fig. 3a, b): at −100 mV, TRPV1 currents only became prominent at temperatures above 40 °C, whereas at +100 mV robust outward currents were already present at room temperature (1,742 ± 279 pA ($n = 17$) versus 59 ± 10 pA ($n = 10$) in non-transfected cells; $P < 0.001$). Thus, similar to TRPM8, the temperature sensitivity of TRPV1 is strongly dependent on the transmembrane voltage.

We then determined how temperature affects the voltage dependence of TRPV1. At 17 °C, significant outward currents could only be measured at potentials above 100 mV, and $V_{1/2}$ was around +150 mV (Fig. 3c–e). Heating induced a gradual leftward shift of the activation curve, resulting in channel activity at more physiological voltages: $V_{1/2}$ decreased by approximately 200 mV upon heating from 17 to 40 °C (9.1 mV °C^{-1}), reaching a value of −50 mV between 40 and 45 °C (Fig. 3e). Thus, heat-induced activation of TRPV1 is the result of a drastic leftward shift of the voltage dependence of activation.

The principle of temperature sensing

Our present results have important implications when considering possible mechanisms for temperature sensing in TRP channels[3]. First, we found that TRPM8 is activated by cooling in cell-free patches. Similarly, previous work has demonstrated heat-activation of TRPV1 in cell-free patches[22]. These results imply that temperature sensing in both channels is a membrane-delimited process, and argue against temperature-dependent binding of second messengers as a mechanism for channel activation. Second, our results demonstrate that temperature-dependent activation of TRPM8 and TRPV1 is not governed by a single characteristic thermal threshold. Temperature sensitivity is modulated by the transmembrane voltage, and changes in ambient temperature result in graded shifts of the voltage dependence of channel activation. These results are not in line with the suggestion that channel activation results from a temperature-dependent phase transition of the lipid membrane or a conformational transition (or denaturation) of the channel protein structure[3], as such processes would predict a single sharp thermal threshold[23].

As an alternative mechanism, we explored whether temperature sensitivity could be the thermodynamic consequence of differences in the activation energies associated with voltage-dependent channel opening and closing. Given that the time course of TRPM8 and TRPV1 currents during voltage steps was mostly well described with a single exponential function, we employed the simplest, two-state model for a voltage-gated channel:

$$\text{Closed} \underset{\beta(V,T)}{\overset{\alpha(V,T)}{\rightleftarrows}} \text{Open}$$

The opening and closing rates α and β are related to membrane voltage and temperature according to[16,24]

$$\alpha = Ae^{-\frac{E_{a,open}}{RT}} e^{\frac{\delta zFV}{RT}} \quad \text{and} \quad \beta = Be^{-\frac{E_{a,close}}{RT}} e^{\frac{-(1-\delta)zFV}{RT}} \qquad (1)$$

©2004 Nature Publishing Group

where $E_{a,open}$ and $E_{a,close}$ represent the activation energies associated with channel opening and closing, R the gas constant ($8.31\,J\,mol^{-1}\,K^{-1}$), T the absolute temperature, z the effective charge associated with voltage-dependent gating, δ is the fraction of z moved in the outward direction, F the Faraday constant ($9.65 \times 10^4\,°C\,mol^{-1}$), V the transmembrane voltage and A and B are preexponential factors. According to Eyring rate theory, activation energy and preexponential factor are related to the enthalpic (ΔH) and entropic (ΔS) component of the activation barrier, according to $E_a = \Delta H + RT$ and $A = k_0 e^{\Delta S/R}$ (where k_0 is the frequency factor)[16,24]. Experimental values for z were obtained by fitting the Boltzmann function to the activation curves (Figs 2d and 3d). Opening and closing rates were obtained from the mono-exponential time constant τ of current activation/deactivation and the steady-state P_{open} using the expressions $\alpha = P_{open}/\tau$ and $\beta = (1 - P_{open})/\tau$ (see Supplementary Fig. S1). Values for α and β as a function of temperature were then displayed in Arrhenius plots (that is, log(rate) versus $1/T$), which allows determination of the activation energy from the slope of the curves.

For TRPM8, the opening rate α was characterized by an $E_{a,open}$ value of 15.7 kJ mol^{-1} corresponding to a 10 °C temperature coefficient (Q_{10}) of 1.2, indicative of a shallow temperature dependence (Fig. 4a). In contrast, the closing rate β was steeply temperature-dependent, reflected in a ~10 times higher value for $E_{a,close}$ of 173 kJ mol^{-1}, which corresponds to a Q_{10} of 9.4 (Fig. 4b). Estimated activation energies were not significantly altered by membrane voltage, which can be appreciated from the parallel Arrhenius plots at different potentials (Fig. 4a, b). Subsequently, we simulated TRPM8 currents using the two-state gating model with the experimentally deduced parameters. Figure 4c shows the simulated temperature dependence of TRPM8 currents at two potentials in response to the cooling ramp used in the experiment of Fig. 2a. The model adequately predicts the cold-induced current activation and the difference in temperature sensitivity at −80 and +100 mV

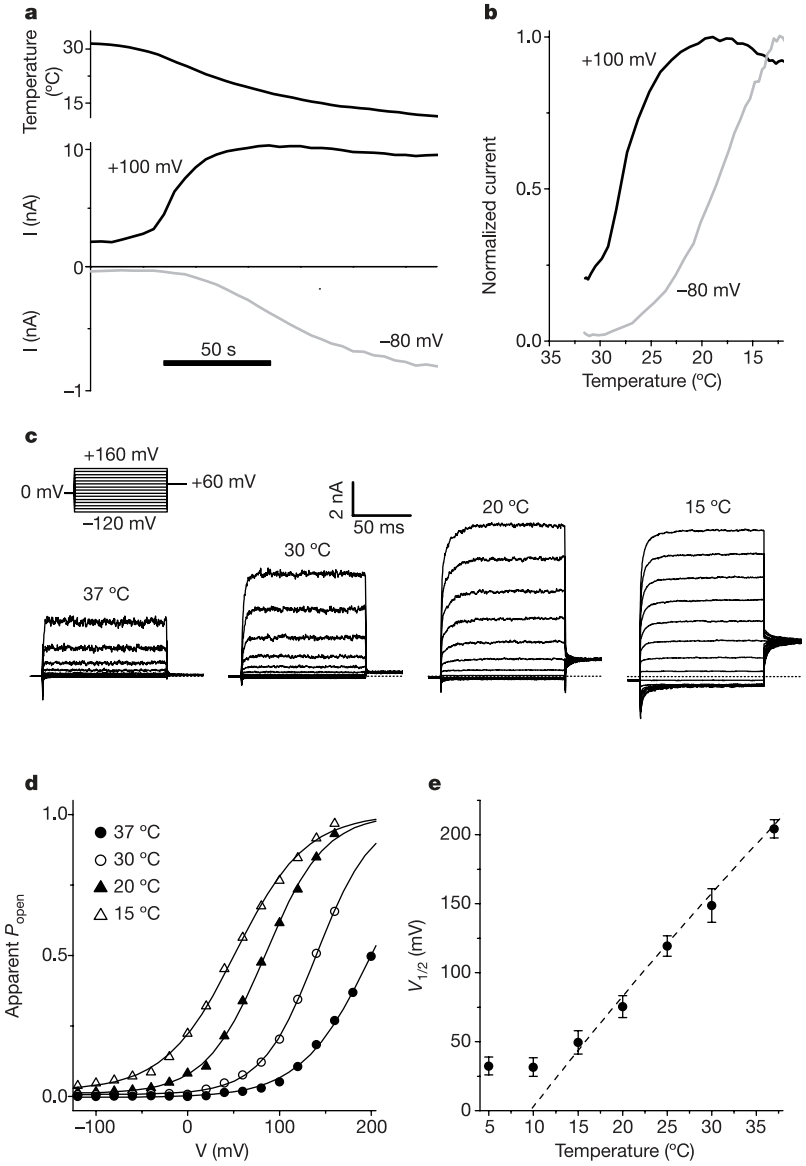

Figure 2 Cooling activates TRPM8 by shifting the voltage dependence of activation. **a**, Whole-cell TRPM8 currents at +100 and −80 mV in response to slow cooling of the bath solution. **b**, Normalized current responses at +100 and −80 mV in function of temperature. **c**, Current traces at different temperatures in response to the indicated voltage protocol. **d**, Steady-state activation curves at different temperatures for the currents shown in **c**. The apparent P_{open} in function of voltage was determined as explained in the methods section. Lines represent Boltzmann functions fitted to the data. **e**, $V_{1/2}$ as a function of temperature (n values between 6 and 15). Dashed line represents the change in $V_{1/2}$ as predicted by the two-state model.

©2004 Nature Publishing Group

(compare Figs 2b and 4c). Likewise, simulated TRPM8 currents in response to voltage steps at different temperatures (Fig. 4d) were strikingly similar to the experimental data (Fig. 2c). Finally, the model predicted the drastic leftward shift of $V_{1/2}$ upon cooling (dashed line in Fig. 2e), except for a small deviation at temperatures below 10 °C, which might reflect channel desensitisation.

In the case of TRPV1, the temperature dependencies of α and β were opposite to those of TRPM8 (Fig. 4e, f): the opening rate α was steeply temperature-dependent ($E_{a,open} = 208\,kJ\,mol^{-1}$; $Q_{10} = 14.8$), whereas the closing rate β showed a shallow temperature dependence ($E_{a,close} = 23.2\,kJ\,mol^{-1}$; $Q_{10} = 1.35$). Using the two-state model with the experimentally deduced parameters, we could faithfully reproduce the temperature dependence of TRPV1 current at different potentials (Fig. 4g), TRPV1 currents in response to voltage steps at different temperatures (Fig. 4h) and the shift of $V_{1/2}$ as a function of temperature (dashed line in Fig. 3e).

The excellent match between model simulations and experimental results for both TRPM8 and TRPV1 led us to formulate a general principle for temperature sensitivity. Temperature sensitivity occurs whenever the activation energies associated with the opening and closing transitions are sufficiently different. When $E_{a,open} \ll E_{a,close}$, the open probability of the channel will increase upon cooling, as illustrated by the behaviour of TRPM8 (Fig. 4a–d). On the contrary, the open probability of the channel will increase upon heating when $E_{a,open} \gg E_{a,close}$, as is the case for TRPV1 (Fig. 4e–h). In most voltage-gated K^+, Ca^{2+} and Na^+ channels the temperature dependence of channel activation and deactivation are similar ($E_{a,open} \approx E_{a,close}$)[16,25,26]. In these channels, increasing temperature leads to an acceleration of channel gating, without major changes in the steady-state open probability.

Although this principle is rather fundamental, we do not exclude that other thermoTRPs exploit different mechanisms. For example, heat activation of TRPV4 does not occur in cell-free patches[5,27], possibly reflecting the necessity of a diffusible messenger. We would also like to point out that a simple two-state model is probably an oversimplification of the full gating intricacies of TRPV1 and

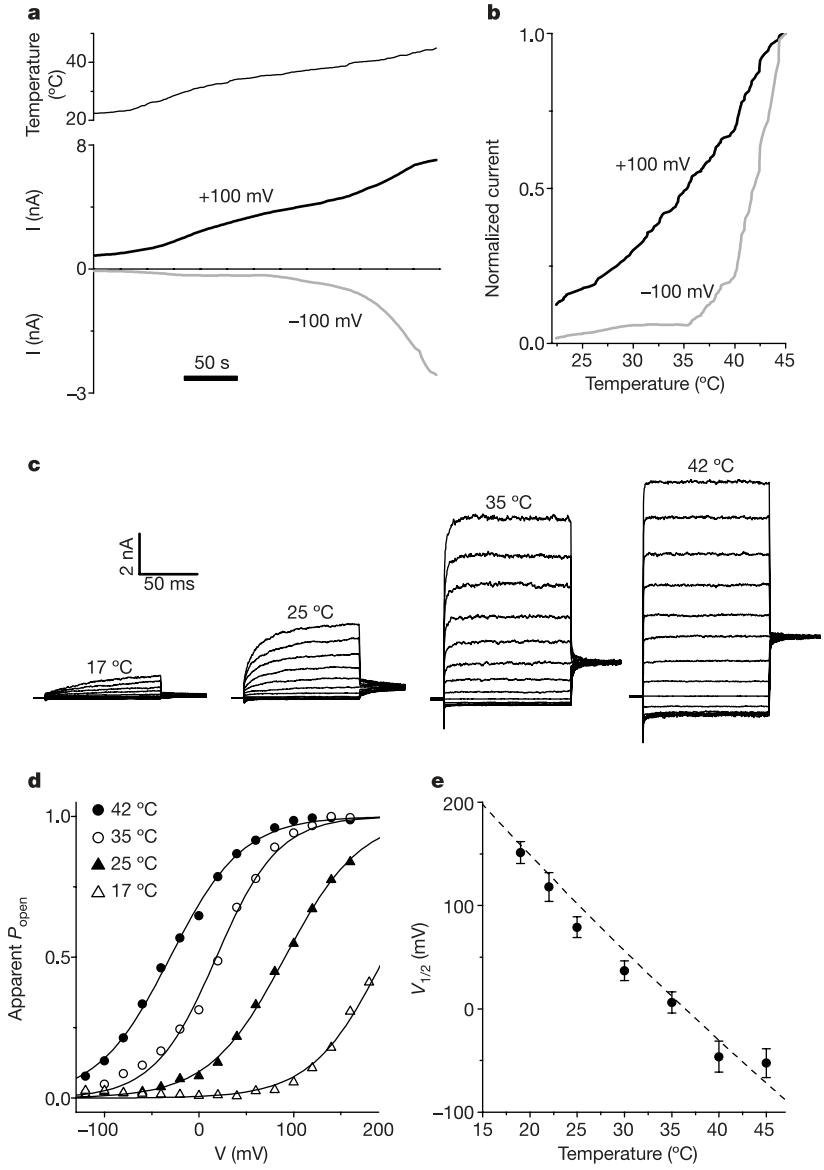

Figure 3 Heating activates TRPV1 by shifting the voltage dependence of activation. **a**, Whole-cell TRPV1 currents at +100 and −100 mV in response to slow heating of the bath solution. **b**, Normalized current responses at +100 and −100 mV as a function of temperature. **c**, Current traces at different temperatures in response to voltage steps ranging from −120 to +160 mV. **d**, Steady-state activation curves at different temperatures for the currents shown in **c**. Lines represent Boltzmann functions fitted to the data. **e**, $V_{1/2}$ as a function of temperature (*n* values between 4 and 9). Dashed line represents the change in $V_{1/2}$ as predicted by the two-state model (see text).

©2004 Nature Publishing Group

TRPM8. Indeed, single-channel measurements of TRPV1 provided evidence for multiple open and closed states[28]. Likewise, we observed that a single exponential function was not always optimal for description of the time dependence of TRPM8, suggesting the presence of more than one open and/or closed state. Nevertheless, the two-state model represents a good approximation of multi-state models as long as the transition with the steepest temperature dependence is rate limiting.

Effect of ligand activators

TRPM8 and TRPV1 not only function as temperature sensors, but also as ionotropic receptors for a variety of chemical substances. TRPV1 is directly gated by several chemicals that cause a burning sensation such as vanilloid compounds and protons[10,22,29], as well as by the endocannabinoid anandamide[30]. In contrast, TRPM8 is activated by several plant-derived and synthetic cooling compounds[12,13,31]. Our present results raised the question whether

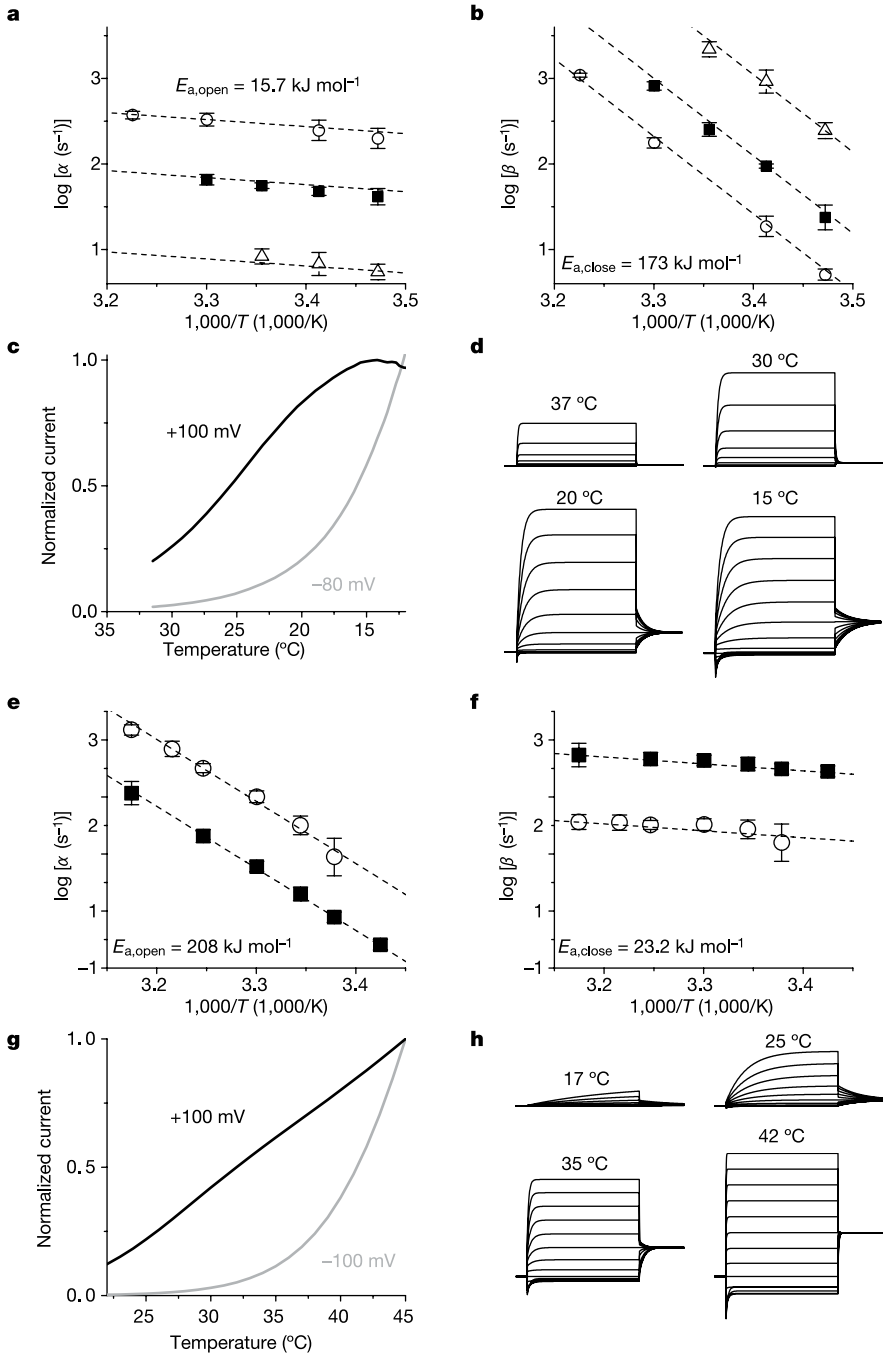

Figure 4 A two-state model accurately predicts the temperature-dependent behaviour of TRPM8 and TRPV1. **a**, **b**, Arrhenius plots of α and β for TRPM8 measured at +160 mV (open circles), +60 mV (filled squares) or −80 mV (open triangles). We obtained the following parameters: $A = 1.37 \times 10^4\,s^{-1}$, $E_{a,open} = 15.7\,kJ\,mol^{-1}$, $B = 1.94 \times 10^{33}\,s^{-1}$, $E_{a,close} = 173\,kJ\,mol^{-1}$, $\delta = 0.5$ and $z = 0.82$. **c**, Simulated TRPM8 current at +100 and −80 mV as a function of temperature. **d**, Simulated TRPM8 currents in response to voltage steps (protocol as in Fig. 2c). **e**, **f**, Arrhenius plots of α and β for TRPV1 measured at +100 (open circles) and −100 mV (filled squares). We obtained the following parameters: $A = 1.61 \times 10^{37}\,s^{-1}$, $E_{a,open} = 208\,kJ\,mol^{-1}$, $B = 9.67 \times 10^5\,s^{-1}$, $E_{a,close} = 23.2\,kJ\,mol^{-1}$, $\delta = 0.5$ and $z = 0.71$. **g**, Simulated TRPV1 currents at +100 and −100 mV as a function of temperature. **h**, Simulated TRPV1 currents in response to voltage steps.

©2004 Nature Publishing Group

these agonists function by modifying the voltage-dependent properties of these channels. To investigate this, we focused on the two best-studied agonists, namely menthol (TRPM8) and capsaicin (TRPV1).

Analogous to previous work[12,13], we found that a low dose of menthol (30 μM) has little effect on inward TRPM8 current at 34 °C, but significantly shifts the cold sensitivity of the channel to higher temperatures (Fig. 5a). The voltage step protocol showed that 30 μM menthol caused a strong potentiation of outward currents, a prominent slowing of tail current deactivation and a significant leftward shift of the activation curve (Fig. 5b, c). The menthol-induced leftward shift of the activation curve was

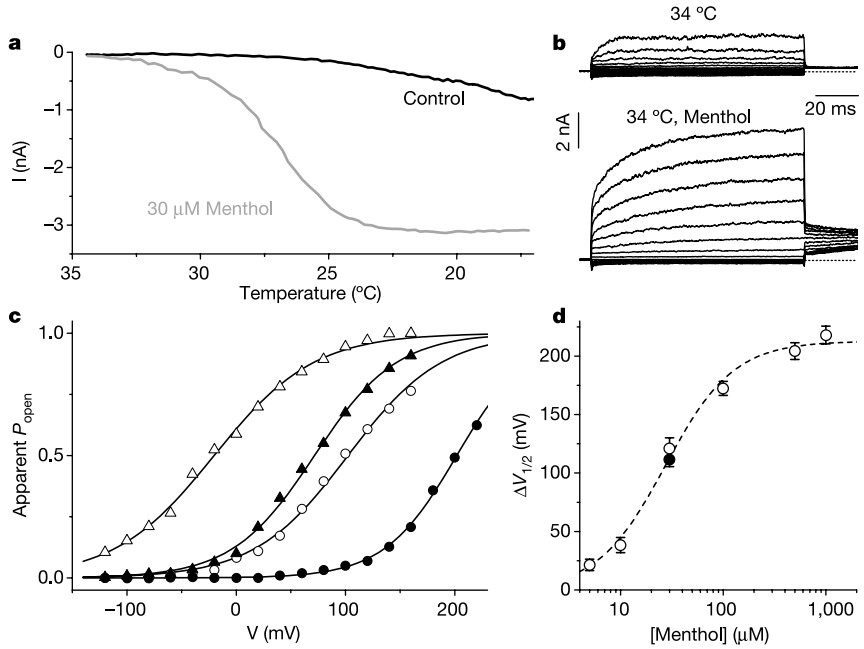

Figure 5 Menthol shifts the TRPM8 activation curve. **a**, TRPM8 currents at −60 mV in response to slow cooling of the bath solution in the absence and presence of 30 μM menthol. **b**, Currents at 34 °C in response to voltage steps ranging from −120 to +160 mV in the absence and presence of 30 μM menthol. **c**, Activation curves at 34 °C (filled symbols) and 24 °C (open symbols) in the absence (circles) and presence (triangles) of 30 μM menthol. **d**, Leftward shift of $V_{1/2}$ ($\Delta V_{1/2}$) as a function of menthol concentration at 32–34 °C (open circles; *n* values between 5 and 20) or 22–24 °C (filled circle; $n = 6$).

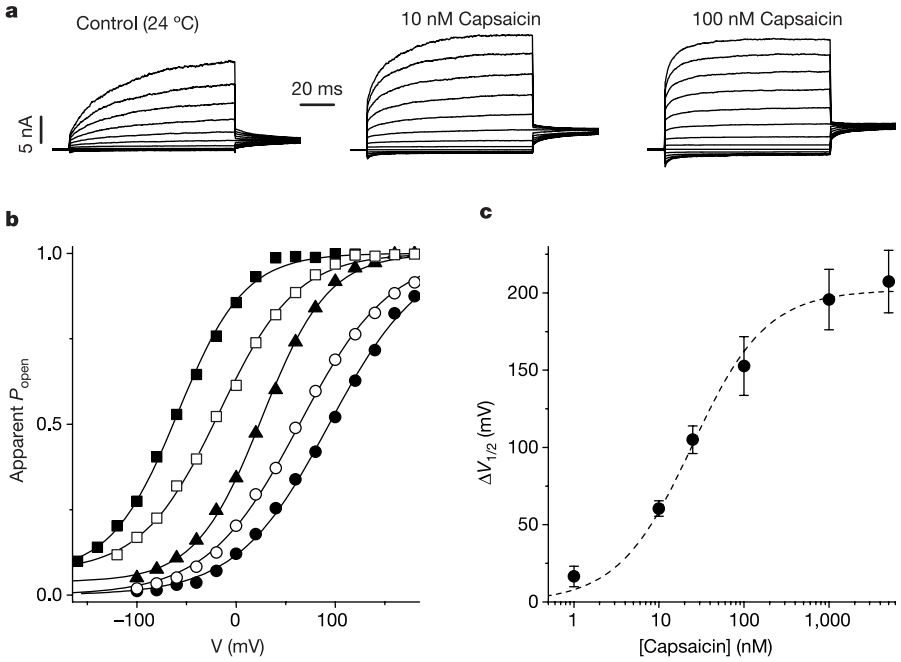

Figure 6 Capsaicin shifts the TRPV1 activation curve. **a**, Currents at 24 °C in response to voltage steps ranging from −100 to +160 mV at the following capsaicin concentrations: 0 nM (closed circles), 1 nM (open circles), 10 nM (closed triangle), 100 nM (open squares) and 1 μM (closed squares). **b**, Steady-state activation curves at 24 °C at the indicated capsaicin concentrations. **c**, $\Delta V_{1/2}$ as a function of capsaicin concentration at 24–26 °C ($n = 4$–10).

©2004 Nature Publishing Group

independent of temperature (Fig. 5c, d), which explains the enhanced cold sensitivity of TRPM8 in the presence of low doses of the cooling agent. The effect of menthol on the activation curve was dose-dependent, with a half-maximal change in $V_{1/2}$ at 27.4 μM (Fig. 5d). Maximal shifts induced by menthol (218 mV at 1 mM; Fig. 5d) were larger than those induced by cooling to 5 °C (Fig. 2e), in line with previous findings showing that menthol is a more efficacious TRPM8 agonist than cold[12].

Capsaicin, the main pungent ingredient of 'hot' chilli peppers, is one of the most potent chemical activators of TRPV1[10,22]. We found that submicromolar concentrations of capsaicin had a robust effect on outward TRPV1 currents at 24 °C, and induced a clear leftward shift of the activation curve (Fig. 6a, b). The effect of capsaicin on the TRPV1 activation curve was dose-dependent, with a half-maximal shift at 28.5 nM and a maximal change in $V_{1/2}$ of ~200 mV (Fig. 6b, c). Note that significant channel desensitisation occurs at capsaicin concentrations >100 nM, which may lead to an underestimation of the shift in $V_{1/2}$ at the highest concentrations tested.

Conclusions

Our results show an unexpected tight link between temperature sensing and voltage-dependent gating in two thermoTRPs with opposite temperature sensitivity. Cold activation of TRPM8 and heat activation of TRPV1 are well described by a single thermodynamic principle, whereby thermosensitivity arises from the difference in activation energies associated with voltage-dependent opening and closing. Chemical agonists of these thermoTRPs function as gating modifiers to mimic and potentiate the thermal responses. At present, the structural determinants of voltage sensing in TRP channels are not known, but the interplay between voltage and temperature sensing implies that any mutational manipulation to the voltage sensor will lead to altered temperature sensitivity. Finally, in a physiological context, our results suggest that the membrane voltage contributes to the fine-tuning of cold- and heat-sensitivity in sensory cells. □

Methods

Electrophysiology

HEK293 were grown in DMEM containing 10% (v/v) fetal calf serum, 4 mM L-alanyl-L-glutamine, 100 U ml^{-1} penicillin and 100 μg ml^{-1} streptomycin at 37 °C in a humidity controlled incubator with 10% CO_2. Cells were transiently transfected with human TRPM8 or human TRPV1 cloned in the bicistronic pCAGGS-IRES–GFP vector using TransIT-293 transfection reagent (Mirus). Between 16 and 24 h after transfection, currents were recorded in the whole-cell or inside-out configuration of the patch-clamp technique using an EPC-9 amplifier and PULSE software (HEKA Elektronik).

Data were sampled at 5–20 kHz and digitally filtered off-line at 1–5 kHz. Between 60% and 90% of the series resistance was compensated, reducing voltage errors to less than 10 mV. The standard intracellular solution for whole-cell measurements contained: 150 mM NaCl, 3 mM $MgCl_2$, 5 mM EGTA and 10 mM HEPES at pH 7.2. The standard extracellular solution contained: 150 mM NaCl, 6 mM CsCl, 1 mM $MgCl_2$, 1.5 mM $CaCl_2$, 10 mM glucose and 10 mM HEPES at pH 7.4. In some experiments, a divalent cation-free extracellular solution was used, which contained 150 mM NaCl, 10 mM EDTA, 10 mM glucose and 10 mM HEPES at pH 7.4. For inside-out measurements, we used the standard extracellular solution in the pipette and the standard intracellular solution in the bath. The temperature of the perfusate was controlled using a SC-20 dual in-line heater/cooler (Warner Instruments). Reported temperature was measured using a TA-29 Thermistor (Thermometrics) placed within 500 μm of the patch-clamped cell.

Data analysis and model simulation

Data analysis, model simulations and data display was performed using Origin 6.1 (OriginLab Corporation) or Igor Pro 4.0 (Wavemetrics). Group data are expressed as mean ± s.e.m. from n cells. The Student's unpaired t-test was used for statistical comparison. Two distinct methods were used to obtain activation curves using the voltage protocol shown in Figs 2c and 3c. In the first approach, tail currents were measured during the first millisecond of the final step +60 mV and normalized to the maximal tail current. However, tail current activation/deactivation at +60 mV was often too fast (time constants <1 ms) for an accurate determination of P_{open}, especially at higher temperatures. In a second approach, steady-state currents at the end of the voltage steps were divided by the estimated fully-activated current–voltage relation of the channel. These open channel current–voltage relations were deduced from tail currents following strongly depolarizing prepulses, similar to the one shown in Fig. 1e, f. In those cases where both approaches were feasible, estimates for $V_{1/2}$ differed by less than 10 mV. For model simulations, we used analytical expressions of P_{open} as a function of temperature, voltage and time for the two-state model. Currents were then calculated assuming a linear conductance and a Q_{10} value for the single-channel conductance of 1.35, similar to that of aqueous diffusion[16].

Received 31 March; accepted 7 June 2004; doi:10.1038/nature02732.

1. Julius, D. & Basbaum, A. I. Molecular mechanisms of nociception. *Nature* **413,** 203–210 (2001).
2. Patapoutian, A., Peier, A. M., Story, G. M. & Viswanath, V. ThermoTRP channels and beyond: mechanisms of temperature sensation. *Nature Rev. Neurosci.* **4,** 529–539 (2003).
3. Clapham, D. E. TRP channels as cellular sensors. *Nature* **426,** 517–524 (2003).
4. Voets, T. & Nilius, B. TRPs make sense. *J. Membr. Biol.* **192,** 1–8 (2003).
5. Watanabe, H. *et al.* Heat-evoked activation of TRPV4 channels in a HEK293 cell expression system and in native mouse aorta endothelial cells. *J. Biol. Chem.* **277,** 47044–47051 (2002).
6. Güler, A. D. *et al.* Heat-evoked activation of the ion channel, TRPV4. *J. Neurosci.* **22,** 6408–6414 (2002).
7. Xu, H. *et al.* TRPV3 is a calcium-permeable temperature-sensitive cation channel. *Nature* **418,** 181–186 (2002).
8. Smith, G. D. *et al.* TRPV3 is a temperature-sensitive vanilloid receptor-like protein. *Nature* **418,** 186–190 (2002).
9. Peier, A. M. *et al.* A heat-sensitive TRP channel expressed in keratinocytes. *Science* **296,** 2046–2049 (2002).
10. Caterina, M. J. *et al.* The capsaicin receptor: a heat-activated ion channel in the pain pathway. *Nature* **389,** 816–824 (1997).
11. Caterina, M. J., Rosen, T. A., Tominaga, M., Brake, A. J. & Julius, D. A capsaicin-receptor homologue with a high threshold for noxious heat. *Nature* **398,** 436–441 (1999).
12. McKemy, D. D., Neuhäusser, W. M. & Julius, D. Identification of a cold receptor reveals a general role for TRP channels in thermosensation. *Nature* **416,** 52–58 (2002).
13. Peier, A. M. *et al.* A TRP channel that senses cold stimuli and menthol. *Cell* **108,** 705–715 (2002).
14. Story, G. M. *et al.* ANKTM1, a TRP-like channel expressed in nociceptive neurons, is activated by cold temperatures. *Cell* **112,** 819–829 (2003).
15. Jordt, S. E. *et al.* Mustard oils and cannabinoids excite sensory nerve fibres through the TRP channel ANKTM1. *Nature* **427,** 260–265 (2004).
16. Hille, B. *Ion channels of Excitable Membranes* (Sinauer Associates, Sunderland, Massachusetts, 2001).
17. Launay, P. *et al.* TRPM4 is a Ca^{2+}-activated nonselective cation channel mediating cell membrane depolarization. *Cell* **109,** 397–407 (2002).
18. Nilius, B. *et al.* Voltage dependence of the Ca^{2+}-activated cation channel TRPM4. *J. Biol. Chem.* **278,** 30813–30820 (2003).
19. Hofmann, T., Chubanov, V., Gudermann, T. & Montell, C. TRPM5 is a voltage-modulated and Ca^{2+}-activated monovalent selective cation channel. *Curr. Biol.* **13,** 1153–1158 (2003).
20. Gunthorpe, M. J., Harries, M. H., Prinjha, R. K., Davis, J. B. & Randall, A. Voltage- and time-dependent properties of the recombinant rat vanilloid receptor (rVR1). *J. Physiol. (Lond.)* **525,** 747–759 (2000).
21. Vlachova, V. *et al.* Functional role of C-terminal cytoplasmic tail of rat vanilloid receptor 1. *J. Neurosci.* **23,** 1340–1350 (2003).
22. Tominaga, M. *et al.* The cloned capsaicin receptor integrates multiple pain-producing stimuli. *Neuron* **21,** 531–543 (1998).
23. Marsh, D. General features of phospholipid phase transitions. *Chem. Phys. Lipids* **57,** 109–120 (1991).
24. Sigworth, F. J. Voltage gating of ion channels. *Q. Rev. Biophys.* **27,** 1–40 (1994).
25. Tiwari, J. K. & Sikdar, S. K. Temperature-dependent conformational changes in a voltage-gated potassium channel. *Eur. Biophys. J.* **28,** 338–345 (1999).
26. van Lunteren, E., Elmslie, K. S. & Jones, S. W. Effects of temperature on calcium current of bullfrog sympathetic neurons. *J. Physiol. (Lond.)* **466,** 81–93 (1993).
27. Chung, M. K., Lee, H. & Caterina, M. J. Warm temperatures activate TRPV4 in mouse 308 keratinocytes. *J. Biol. Chem.* **278,** 32037–32046 (2003).
28. Liu, B., Hui, K. & Qin, F. Thermodynamics of heat activation of single capsaicin ion channels VR1. *Biophys. J.* **85,** 2988–3006 (2003).
29. Jordt, S. E., Tominaga, M. & Julius, D. Acid potentiation of the capsaicin receptor determined by a key extracellular site. *Proc. Natl Acad. Sci. USA* **97,** 8134–8139 (2000).
30. Zygmunt, P. M. *et al.* Vanilloid receptors on sensory nerves mediate the vasodilator action of anandamide. *Nature* **400,** 452–457 (1999).
31. Behrendt, H. J., Germann, T., Gillen, C., Hatt, H. & Jostock, R. Characterization of the mouse cold-menthol receptor TRPM8 and vanilloid receptor type-1 VR1 using a fluorometric imaging plate reader (FLIPR) assay. *Br. J. Pharmacol.* **141,** 737–745 (2004).

Supplementary Information accompanies the paper on **www.nature.com/nature**.

Acknowledgements We thank K. Talavera, G. Owsianik, J. Vriens, F. Mahieu and J. Prenen for helpful suggestions and criticisms, and C. Benham (GlaxoSmithKline) for providing us with the human TRPV1 clone. This work was supported by the Belgian Federal Government, the Flemish Government and the Onderzoeksraad KU Leuven. T.V. is a postdoctoral Fellow of the Fund for Scientific Research, Flanders (Belgium) (FWO-Vlaanderen).

Competing interests statement The authors declare that they have no competing financial interests.

Correspondence and requests for materials should be addressed to T.V. (Thomas.Voets@med.kuleuven.ac.be).

©2004 Nature Publishing Group